Adhesively Bonded FRP Reinforcement of Steel Structures: Surface Preparation Analysis and Influence of the Primer

Quentin Sourisseau, Emilie Leprêtre, Sylvain Chataigner, Xavier Chapeleau, Luc Mouton, Stéphane Paboeuf

Proceedings of the ASME 2022 41st International Conference on Ocean, Offshore and Arctic Engineering
OMAE2022
June 5-10, 2022, Hamburg, Germany

OMAE2022-XXXX

ADHESIVELY BONDED FRP REINFORCEMENT OF STEEL STRUCTURES: SURFACE PREPARATION ANALYSIS AND INFLUENCE OF THE PRIMER

Quentin Sourisseau
University Gustave Eiffel, MAST-SMC Bouguenais, France, University Gustave Eiffel, Inria, COSYS-SII, I4S Team, Bouguenais, France, Bureau Veritas Marine & Offshore, Environment & Technologies Department, Nantes, France

Emilie Leprêtre
University Gustave Eiffel, MAST-SMC Bouguenais, France

Sylvain Chataigner
University Gustave Eiffel, MAST-SMC Bouguenais, France

Xavier Chapeleau
University Gustave Eiffel, Inria, COSYS-SII, I4S Team, Bouguenais, France

Luc Mouton
Bureau Veritas Marine & Offshore, Environment & Technologies Department, Nantes, France

Stéphane Paboeuf
Bureau Veritas Marine & Offshore, Environment & Technologies Department, Nantes, France

ABSTRACT

In tropical areas, with marine environment, high temperature and humidity, corrosion is a constant threat. The maintenance of steel structures (like FPSO's) is becoming a challenge. The current technique of "crop and renewing" repair involves a certain number of major issues for project owners such as: "hot work", that is to say welding; temporary weakening of the structure; need to empty, clean and purging the oil tanks of the FPSO's, resulting in long downtime and an expensive solution. "Cold repair", such as composite repair, is a promising solution. However, surface preparation and the influence of the primer are crucial issues to be addressed to ensure the strength and reliability of this type solution based on bonded patch.

The paper presents an experimental study of the influence of the surface preparation and the primer on the strength of small steel bonded specimens which have been deliberately degraded by corrosion and pollution. Several surface preparation methodologies were investigated and the quality of these preparations was assessed using methods that can be implemented on site. Two main aspects were investigated: the detection of the residual presence of pollutants through the use of a portable infrared spectrometer; and the determination of surface energy after preparation using contact angle and wettability measurement equipment. To study the impact of the primer on the adhesion capacity of the steel surface, critical toughnesses measurements was performed with End notch flexure tests. Three configurations have been tested: bonding with the epoxy resin without initial application of primer and bonding with the Epoxy resin with initial application of two Primer A and B. The results shown clearly that the type of primer and the quality of its application are paramount importance to ensure the strength of steel bonded patches.

1. INTRODUCTION

FPSOs (Floating Production Storage and Offloading units) and large ships are so far mainly made of steel. For both structures, corrosion is a permanent threat in marine environment. New repair/reinforcement techniques for these structures are currently under development, in particular glued laminated repair solutions such as FRP (Fibre Reinforced Polymer)

patches which have several advantages (short downtime and non-intrusive process) [1]. The repair of a corroded ship deck imposes significant constraints on the design. The patch may indeed be located in an area that is entirely subject to the deformation of the ship's beam causing high stresses on the edges of the patch. The need to ensure maximum adhesion in these areas is therefore paramount. In adhesive bonding operations, this is most of the time reached through adequate surface preparation. To be able to mitigate the risks of local poor surface preparation, efficient surface control methodologies are needed. Besides, the application constraints (especially for offshore operations) may require the use of primers to cope with the necessary delays between surface preparation operations and FRP application. It is thus momentous to verify the impact of such primer application on the obtained adhesion. The presented study is concerned with those two issues.

The first part of the paper is dedicated to the presentation of experimental investigations realized on different surface preparations [2] of steel specimens. Some of them have been deliberately degraded by corrosion and pollution (similar to that present on FPSOs and ships) Two main aspects were investigated: the detection of the residual presence of pollutants, using a portable infrared spectrometer [3]; and the determination of surface energy, after preparation, using contact angle and wettability measurement equipment [4]. The second part of the paper concerns with the influence of the primer on the obtained adhesion of the FRP reinforcement. End Notch Flexure (ENF) tests [5] were performed for three configurations (one without primer and two with different primers). The results were used to define an application protocol for a FRP bonded reinforcement, and the needed on-site control operation.

2. SURFACE PREPARATION ANALYSIS

2.1. Studied specimens and initial pollution

As shown in Fig. 1, thirteen specimens were used for this study and consisted in S235 steel plates (yield strength: 235 MPa). Each specimen was treated as follows (Figure 11):

- initial grid blasting, to remove iron oxide from the steel plate and start the ageing process with clear bare steel,
- ageing for two days in an outdoor environment (humidity > 95%) to create a corrosion layer on the surface,
- pollution of the surface of the specimens with: diesel (four specimens), hydraulic oil (four specimens) or a paraffinic corrosion protection spray (four specimens). Those pollutants are considered to be the most encountered one for the studied application. Two specimens were left unpolluted and serve as a reference,
- after the pollution of each sample, two more days of ageing in an outdoor environment (humidity > 90%) were observed to recreate a corrosion layer.

Figure 1: SPECIMENS USED FOR THE SURFACE PREPARATION ANALYSIS AFTER AGEING AND POLLUTION.

2.2. Surface preparations

Four types of surface treatment were carried out for each type of pollution:

- preparation (A): detergent cleaning,
- preparation (B): detergent cleaning, followed by sandblasting and the application of an anti-corrosion primer (*A*),

- preparation (C): detergent cleaning, followed by sandblasting, solvent cleaning and the application of an anti-corrosion primer *A*,
- preparation (D): detergent cleaning, followed by sandblasting and solvent cleaning.

The pollution by diesel, hydraulic oil, or paraffin spray were respectively named (1), (2) and (3) while the pollution-free samples were named (4). The different surface preparations of each specimen shown in Fig. 2 are summarized in Table 1.

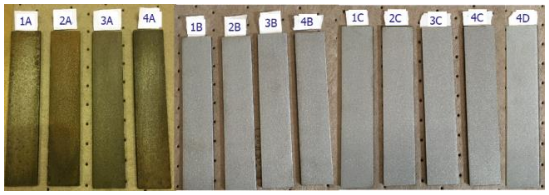

Figure 2: SPECIMENS AFTER SURFACE PREPARATION

Preparation of surface / Type of pollution	A detergent	B detergent + blasting + primer A	C detergent + blasting + solvent + primer A	D detergent + blasting + solvent
1 diesel	1A	1B	1C	-
2 hydraulic oil	2A	2B	2C	-
3 paraffin spray	3A	3B	3C	-
4 no pollution	4A	4B	4C	4D

Table 1: SPECIMENS REFERENCING

2.2.1. Pollution analysis using infrared spectrometry

In order to investigate the ability of the different surface preparations to remove the initially deposited pollutants, an infrared spectrometer (Agilent Technology 4300 [3]) was used. Fig.3 shows a comparison of the absorption spectra curves obtained for the specimens with type (A) surface preparation (specimens 1A, 2A, 3A, 4A) and the clean reference specimen with type (D) surface preparation (specimen 4D). It is important to mention that these curves have been artificially shifted in ordinates to better distinguish them

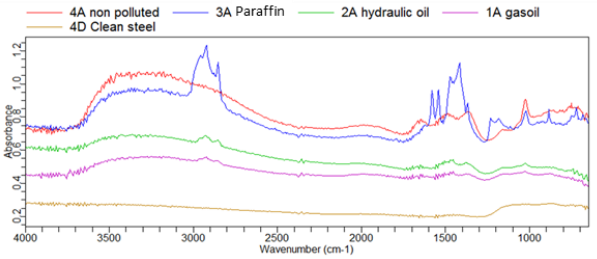

Figure 3: INFLUENCE OF INITIAL POLLUTION ON INFRARED SPECTROMETER MEASUREMENTS FOR TYPE (A) SURFACE PREPARATION.

Fig. 3 shows the presence of rust (local peak between 3000 and 3500 cm^{-1}) on specimens 1A, 2A, 3A and 4A, as well as the presence of more or less marked pollution (peaks between 2800 and 3000 cm^{-1} and peaks between 1200 and 1700 cm^{-1}) for the specimens 1A, 2A and 3A. As a result, it confirms with the visual inspection that, cleaning with detergent alone does not seem sufficient to remove completely rust and pollution. Interestingly, the use Fourier Transform infrared spectroscopy (FTIR) technique that is easily movable on site can be used for surface control operations before bonding.

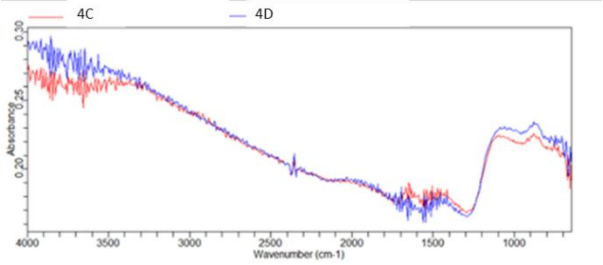

Figure 4: INFLUENCE OF THE PRESENCE OF PRIMER ON INFRARED SPECTROMETER MEASUREMENTS.

Fig.4 shows the absorption curves for the references specimens (4D) before and after the primer *A* application. As it can be seen, the presence of primer *A* does not affect the absorbance measurements enough (between 500 and 4000 cm^{-1}) for the FITR to

be considered as an efficient measurement technique to control the primer *A* application on steel surface.

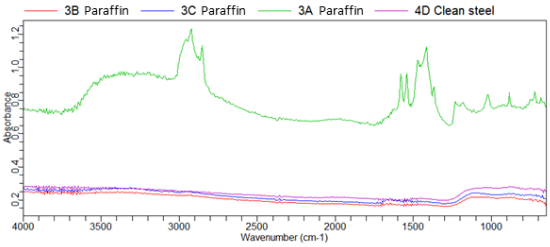

Figure 5: COMPARISON OF THE INFRARED SPECTRA OBTAINED FOR THE THREE SURFACE PREPARATION METHODS STUDIED AND THE PARAFFIN TYPE POLLUTION.

Finally, Fig. 5 shows a comparison of the absorption curves obtained for the specimens (3A), (3B), (3C) and (4D). It can be observed that the surface preparation of type (B), (C) and (D) (with a sandblasting, follows or not by a solvent cleaning) give similar infrared spectra indicating adequate (no detection) removal of the pollutant. Given that the presence of the primer *A* shows very little effect on the measurement as mentioned above (see Fig3.). it can be concluded that sandblasting allows removing rust (which becomes undetectable in the FTIR analysis), but also the paraffin pollution since it is no longer detectable in the FTIR analysis after sandblasting, whether or not solvent degreasing has been carried out. It therefore seems that solvent cleaning after sandblasting is not necessary to eliminate residual pollutants. Similar results were obtained for the others pollution (diesel and hydraulic oil).

2.2.2. Surface energy measurements

The molecular force of attraction between different materials is related to their surface properties (surface energy and/or surface tension) and conditions their adhesion. For a solid, a high surface energy means a strong molecular attraction, while a low surface energy results in lower forces of attraction. For optimum bonding of two materials, it is interesting to optimize wettability (liquid on solid). This results most of the time in a higher surface energy of the solid (substrate to be bonded) than of the liquid (adhesive) [3].

In this study, surface energy measurements were carried out using two techniques that may be carried on site:

- The WCA "Water Contact Angle" technique [4]. This technique was carried out using a thermoregulated tensiometer (Kruss DSA100) and 3 reference liquids (water, ethylene glycol, glycerol) deposited in drop on the studied surfaces (Fig. 6). It should be noted that some of the used liquids (ethylene glycol and glycerol) led to a dissolution of the primer *A*. Those measurements could therefore not be processed and analyzed.
- Spread measurements using wettability measurement inks (Fig. 7). The used inks have a measuring range of 31 to 67 mJ/m² with a step between each ink of 2 mJ/m² (any values outside this range cannot be precisely measured).

Figure 6: CONTACT ANGLE MEASUREMENT

Figure 7: USE OF SPREAD MEASURING INKS.

For both techniques (except for high energies for which the used inks were not adapted), it was observed that the surface energy measurements are similar for test specimens having the same surface preparation and whatever the pollution. For this reason, only the range of surface energy measurements for the different surface preparation are given in table 2.

Specimens	Wettability ink (mJ/m²)	Contact angle measurement (mJ/m²)
B and C (with primer *A*)	36 - 44	40 ± 12
D (without primer *A*)	67+	90 ± 10

Table 2: SURFACE ENERGY MEASUREMENT RESULTS.

Interestingly, similar results were obtained for both surface energy measurement techniques (except for high energies for which the used inks were not adapted). With surface treatment B, C, D, it appears that it is not possible to clearly differentiate between polluted test specimens. It also appears that sandblasting followed by cleaning with solvent (preparation D, compare to A) significantly increases surface energy. Yet, the comparison of the surface energies obtained for the type C and D surface preparations shows that the application of an anti-corrosion primer on the sandblasted surface strongly reduces significantly (from 30% to 60%) the surface energy and thus the adhesion between the bonded surfaces. Therefore, some mechanical tests will allow to better evaluate the influence of the primer application on the strength of the bonding.

3. MECHANICAL INVESTIGATIONS RELATED TO THE USE OF A PRIMER

3.1. Studied samples

In order to be sure that the application of a primer does not affect badly the value of the critical toughness, tests were done considering the three following configurations:

- bonding with the epoxy resin without initial application of primer,
- bonding with the epoxy resin with initial application of two Primer *A* and *B*

The samples were made following the surface preparation C for the specimen (2) and (3) and the surface preparation D for the specimen (1). The rugosity was measured (Ra between 5µm and 8µm). The primer application of the primer *B* has been made with a roller (Fig. 8). The primer *A* with a lint free cloth (Fig. 8 B, C, as recommended by the manufactures of the two primers). The adhesive application was done by dropping the resin between the two surfaces (one on each adherent), then the samples were cured at room temperature during 6 hours, and finally post-cured at 70°C during 12 hours as recommended by the epoxy manufacturer.

In the following analysis, only the mode II fracture is considered since it is the preponderant mechanism of fracture for bonded reinforcements on steel structures. The samples geometry is inspired by the standards related to the ENF tests for the determination of composites fracture toughness in mode II [5]. The standard samples geometries, proposed for unidirectional CFRP laminate, have been up-scaled in relation with the adherent thickness of 6mm and the substrates have been modified by steel plates. The specimens were made with two 900MPa rolled steel plates (thickness 5 mm, manually bonded to obtain a 1mm thick bondline). The initial crack was obtained by adding Teflon insert on one of the adherents to create the correct initial crack length, a_0 (distance between one of the supporting rollers during the test and the crack front, Fig. 10**Figure 9**).

A) **B)**

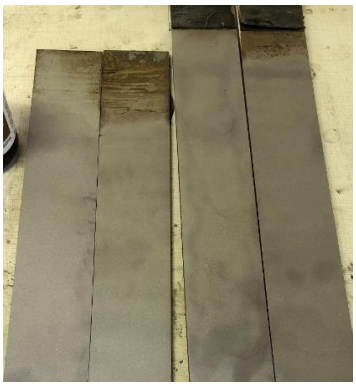

C)

Figure 8: A) PRIMER *B* APPLICATION WITH A ROLLER **B)** PRIMER APPLICATION WITH THE LINT FREE CLOTH, **C)** PRIMER *A* APPLIED IN THIN LAYER.

The nomenclature of the specimens is as follows: specimens III and IV for configuration (1); specimens V and VI for configuration (2); and specimens I, II for configuration (3) (Tab 4.). For each specimen, number -1 or -2 was also specified corresponding to the tested side of the specimen (specimens were manufactured in order to have the two sides that can be tested). It should be noted that the DIC monitoring was not successful for tests I-1 and I-2 and sample V-2 broke before testing. Therefore, none of the results depending of this instrumentation of these tests will be presented.

Specimens Configuration	1 bonding without primer	2 bonding with primer *A*	3 bonding with primer *B*
Specimens referencing	III 1 III 2 IV 1 IV 2	V 1 V 2 VI 1 VI 2	I 1 I 2 II 1 II 2

Table 4: REFERENCING OF SPECIMENS USED FOR MECHANICALS TESTS

3.2. Description of the realized tests: ENF

The overall geometries of all the samples are resumed in the Fig. 9 and Tab. 4.

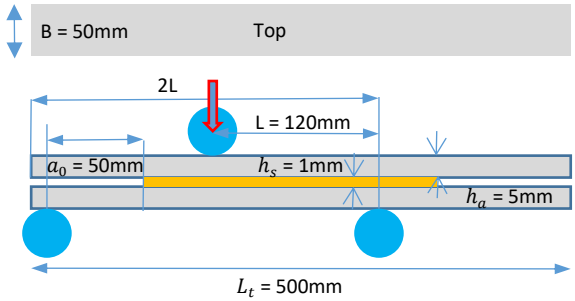

Figure 9: ENF TEST SAMPLE GEOMETRY

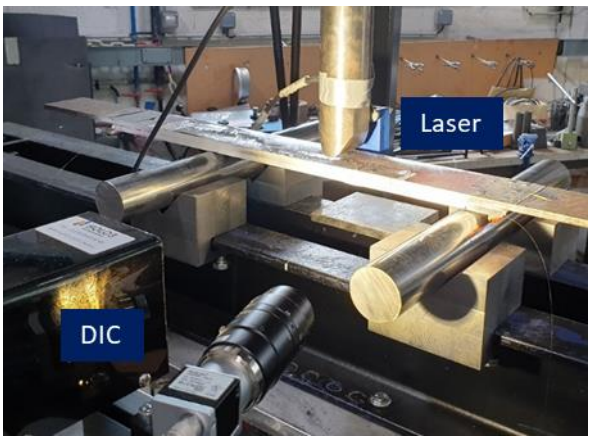

Figure 10: PHOTO OF ONE OF THE ENF TEST

As visible in the picture of Fig. 10, three systems of monitoring were used during the test campaign:

- A digital image correlation device used for surface displacements measurement closed to the crack tip,
- a laser used for the load application point displacement measurement,
- a load cell (capacity $50\,kN\ +-0.145\%$) used for the applied load measurement.

The used optical set-up was composed of two Basler acA2440-75um cameras (5 Mpx sensor) with two 50mm Kowa LR1015WM52 lenses with a stereo angle of 15 degrees placed at a distance of around 30±1cm of the sample. The acquisition rate was set at 5Hz. A black and white speckle has been deposited on the test specimen by non-homogeneous spraying of paint in three successive layers (white / black / white) with an approximative pattern size of (visually obtained) of around 0.2 mm. A commercial system (CorreliSTC by Corelli Solution, [6]) was used to carry out digital image stereo-correlation on one of the two flanks where the border of the crack front is visible ~~(ENF)~~.

3.3. Toughness determination and results

The critical toughness values for the ENF tests were obtained with the J-integral approach and the ASTM D7905 standard computation method. The standard proposes to use the Compliance Calibration Method (CCM) with the equation (1) to express the compliance (C = Displacement / Load) of the ENF assembly as a cubic function of the crack length a.

$$C = D + ma^3 \quad (1)$$

With D and m constant values.

The critical toughness G_{IIC} is expressed with equation 2 for a sample of width B.

This approach requires calibration of compliance as a cubic function of crack length, done with multiple samples (at least 3) with different initial crack lengths a_0. Moreover, it assumes that crack propagation only takes place when the force has reached its peak P_{max} (the load corresponding to crack onset).

The above method can only be used in cases when linear elastic fracture mechanics (LEFM) theory can be applied, which assumes that there is limited material non-linearity in the adhesive. Therefore, this analysis neglect the impact of the process zone upstream of the crack front. This can lead to inaccurate G_{IIc} for materials that develop a rather large process zone compared to the overall size of the samples.

The J-integral is a technique used for calculating the fracture energy for problems where the assumptions of the LEFM are no longer valid. It is defined by a contour integral whose value is equal to the energy release rate. Rice [7] has shown that for monotonic loading with crack propagation occurring in homogenous material, the J-integral is path independent and its value is equal to the energy released during the damage process for linear and nonlinear elastic body ($J_{crit} = GIIc$). Those two properties allow us to select the most convenient path to integrate the stresses and to compute the energy release rate from common tests, as the ENF one. Leffler [8] proposed a simplified expression of the J-integral based on LFEM, taking into account the substrate strain and shear strain in the adhesive for the ENF test.

$$J_{ENF} = \frac{9}{16}\frac{(Pa_0)^2}{E{h_s}^3B^2} + \frac{3\delta_s}{8h_sB} \quad (3)$$

With P the load, a_0 the initial crack length, δ_s the local sliding (see Fig. 11), E the adherent Young's modulus, h_s the adherent thickness and B the sample width.

The first term of the above equation corresponds to the classical beam theory considering a rigid adhesive while the second term corresponds to the effect of the flexibility of the adhesive. To be applied, a long enough distance between the crack tip and the loading point must be ensured to avoid

$$G_{IIC,ASTM} = \frac{3{P_{max}}^2 m{a_0}^2}{2B} \quad (2)$$

any impact of the local stress concentration of the application point in the bondline.

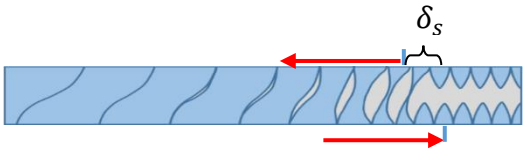

Figure 11: ENF LOCAL SLIDING AT THE CRACK FRONT.

The resulting curves are described in Fig. 12, Fig. 13, and Fig. 14.

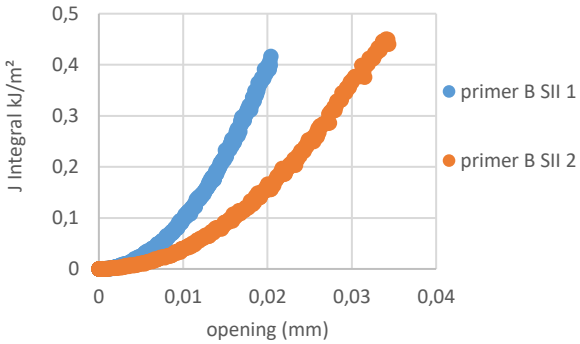

Figure 12: J-INTEGRAL COMPUTATION FOR THE TEST WITH THE PRIMER *A*

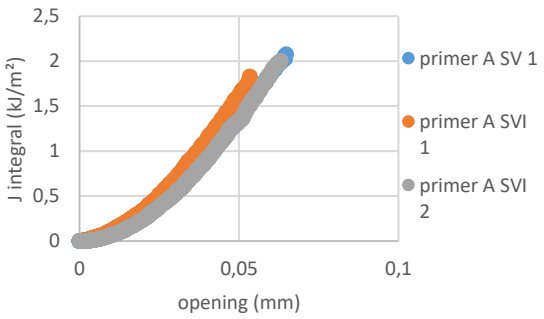

Figure 13: J-INTEGRAL COMPUTATION FOR THE TEST WITH THE PRIMER *A*

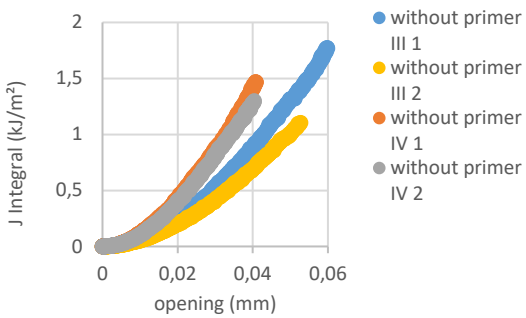

Figure 14: J-INTEGRAL COMPUTATION FOR THE TEST WITHOUT PRIMER

The curves described to local energy lost around the crack tips up to the point of crack propagation. The maximal value J_{crit}, is the maximal energy stored before the crack propagation at the crack tips which is equal to the critical toughness of the bonding.

Tab. 5 and Tab. 6 describe the obtained critical toughnesses with, respectively, the J-integral approach and the standard computation method.

Critical toughness (kJ/m²)\ surface preparation	Without primer Tests: III-1 III-2 IV-1 IV-2	Primer *A* Tests : VI-1 VI-2 VI-1 VI-2	Primer *B* Tests : II-1 II-2 I-1 I-2
	1.90	2.05	0.41
	1.12	1.90	0.45
	1.49	2.01	
	1.35		
Average	1.46	1.99	0.43

Table 3: CRITICAL TOUGHNESS COMPUTATION FOLLOWING THE J-INTEGRAL

Critical toughness (kJ/m²) \ surface preparation	Without primer Tests: III-1 III-2 IV-1 IV-2	Primer *A* Tests : VI-1 VI-2 VI-1 VI-2	Primer *B* Tests : II-1 II-2 I-1 I-2
	1.73	2.15	0.34
	3.20	2.51	0.36
	2.59	2.21	0.70
	2.37		0.53
Average	2.47	2.29	0.48
Standard deviation	60%	18%	14%

Table 4: CRITICAL TOUGHNESS COMPUTATION FOLLOWING THE ASTM D7905 STANDARD.

Independently of the critical toughness computation method, the results with the primer *B* (Fig. 13) are much lower (~0.5kJ/m²) compared to the results with the primer *A*, and without any primer (1.5+ kJ/m²) as shown in Fig. 15 A and B. The results also shows that the primer *A* with the Epoxy resin adhesive does not decrease the critical toughness. The limited number of tests does not allow a high confidence into the values of standard deviation. However, it is to be noted that the results with primers seems to have a lower dispersion in comparison with the results without primer (see Fig 15 A and B). In addition, the analysis on the two computation methods show that the results are similar for both primers with values around 0.5 kJ/m² and 2 kJ/m². The results for the tests without primer are quite different with values of 2.5 kJ/m² with the ASTM computation method, and 1.4 kJ/m² with the J-integral computation method.

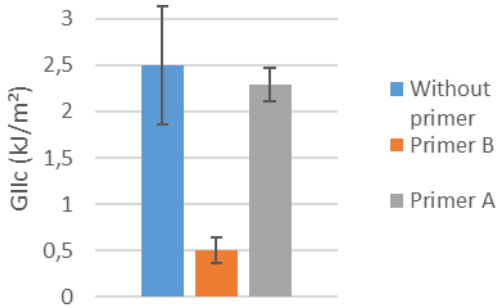

A)

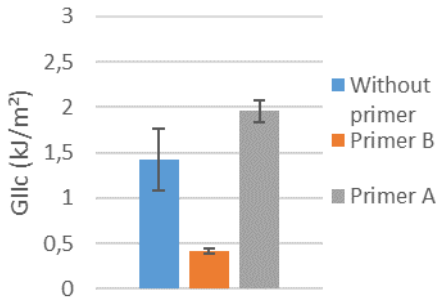

B)

Figure 15 : A) ASTM CRITICAL TOUGHNESS COMPUTATION, **B)** J-INTEGRAL CRITICAL TOUGHNESS COMPUTATION

4. CONCLUSION

The presented investigations focused on the comparison of different surface preparation methods and the influence of primer application.

Surface preparation analysis was carried out for determining two main characteristics: surface FTIR measurements, and wettability assessment. For all the studied pollutants corresponding to the main ones being encountered for the studied application, the results were similar. Sand blasting seems to be needed (and enough) to remove existing pollutants, and to obtain high surface energies (multiplication by three). Regarding the primer, it was not possible to detect it using FTIR, and its presence proved to degrade surface wettability. It was then decided to proceed to mechanical destructive testing to analyze its effect on the adhesively bonded joint resistance.

This work was carried out determining mode II toughnesses through ENF tests. The critical toughness obtained with primer *A* remained similar to the one obtained without primer. This tends to indicate that, though this primer tends to decrease surface wettability, additional adhesion mechanisms allow obtaining similar toughness characteristics. This is not the case for primer *B* for which a high decrease of the toughness was observed (divided by 4). When using a primer, its choice and the quality of its application are therefore momentous for the success of the adhesion. More investigation are needed regarding the tolerances related to primer application.

ACKNOWLEDGEMENTS

This study is supported by Strength Bond project The authors would like to acknowledge all the partners: Bureau Veritas, Total Energies, Petrobras, Siemens, Naval Group, Infracore Compagny and Coldpad (https://marine-offshore.bureauveritas.com/strength-bond-offshore-assessing-strength-bonded-repairs)

REFERENCES

[1] Sourisseau, Q., Leprêtre, E., Chataigner, S., Chapeleau, X., Mouton L., Paboeuf S., “Use Of Distributed Optical Fibre To Monitor The Crack Propagation Of An Adhesively Bonded Joint During An ENF Test”. CICE 2020 Istanbul.

[2] NF EN ISO 8503- Preparation of steel substrates before application of paints and related products - Surface roughness characteristics of blast-cleaned steel substrates - method for the grading of surface profile of abrasive blast-cleaned steel, April 2012.

[3] Agilent technical datasheet, https://www.agilent.com/cs/library/flyers/public/5991-4123EN_Flyer_4300_MCT.pdf, 2014.

[4] Boulangé, L., Bonin, E., Saubot, M., “Physicochemical characterisations of the bitumen – aggregate interface to get a better understanding of stripping phenomena”. Road Mater. Pavement Des., 2013 :37–41.

[5] D7905 Standard test method for determination of the mode II interlaminar fracture toughness of unidirectional fiber-reinforced polymer matrix composites. West Conshohocken, PA: ASTM International. 2014.

[6] https://www.correli-stc.com/

[7] Rice J., “A path independent integral and the approximate analysis of strain concentration by notches and cracks”. Journal of Applied Mechanics. 1968;35:379-386.

[8] Leffler, K., Alfredsson, S., Stigh, U., “Shear behavior of adhesive layers”. International Journal of Solids and Structures. 2006;44.